Electronic Supporting Information (ESI)

Cobalt and nitrogen co-doped hierarchically porous carbon nanosheet as bifunctional electrocatalys for oxygen reduction and evolution reactions

Jakkid Sanetuntikul[a,b], Suyeon Hyun[a], Pandian Ganesan[a], and Sangaraju Shanmugam [a]*

[a] Department of Energy Science & Engineering, Daegu Gyeongbuk Institute of Science & Technology (DGIST), Daegu, Republic of Korea, 42988

[b] Faculty of Engineering and Technology, King Mongkut's University of Technology North Bangkok (KMUTNB),Bankhai, Rayong, Thailand, 21120

E-mail: sangarajus@dgist.ac.kr

Experimental

Physical characterization analysis:

The microstructures of samples were determined by field-emission transmission electron microscope (FE-TEM, Hitachi, HF-3300) with an acceleration voltage of 300 kV. For TEM analysis, samples were ultrasonically dispersed in isopropyl alcohol (IPA), and then a drop of dispersion was deposited on copper grid and dry under UV lamp. The crystal structure of samples was investigated by powder X-ray diffraction (XRD, Panalytical-Empyrean) using Cu Kα radiation at a generator voltage of 40 kV and a tube current of 30 mA. The N_2 adsorption-desorption measurements were carried out using 'Micromeritics' (ASAP 2020) at 77 K. Bruner-Emmett-Teller (BET), Barrett-Joyner-Halenda (BJH) models were used to determine the specific surface area, the mesoporous (2-50 nm) pore size distributions information for the CoAAC samples. Before the measurements, the samples were degassed at 200 °C under vacuum for 4 hours. Crystal structure and elemental analysis studies performed by X-ray photoelectron spectroscope (XPS, Thermo Fisher Scientific, ESCALAB250 XPS system, Theta Probe XPS system) using monochromated Al K-alpha source at 15 kV and 150 W. Binding energy values at X-axis were calibrated using C1s from a carbon value taken as 284.6 eV.

Electrochemical characterization analysis:

The slopes of ORR for RDE based on Koutecky-Levich plots were determined by follow equation.

$$\frac{1}{J} = \frac{1}{J_L} + \frac{1}{J_K} = \frac{1}{B\omega^{\frac{1}{2}}} + \frac{1}{J_K}$$

$$B = 0.62\, n\, F\, C_0\, D_0^{\frac{2}{3}}\, v^{-\frac{1}{6}}$$

Where, J is the experimentally measured current, JL is the diffusion-limiting current, JK is the kinetic current, ω is the angular velocity, F is the Faraday constant, C_0 is the saturated concentration of O_2 in 0.1 M KOH (1.2×10^{-6} mol cm^{-3}), D_0 is the diffusion coefficient of O_2 in 0.1 M KOH (1.9×10^{-5} cm^2 s^{-1}), and ν is the kinematic viscosity of the electrolyte. "n" can calculate from slop by under plot of J^{-1} vs $\omega^{-1/2}$ and J_k is calculated from inverse of intercept.

For RRDE, the formation of HO_2^- and the electron transfer number were determined by follow equation;

$$OH_2^- (\%) = 200 \times \frac{I_R / N}{I_D + (I_R/N)}$$

$$n = 4 \times \frac{I_D}{I_D + (I_R/N)}$$

Where, I_D is the disk current, I_R is the ring current, and N is the ring correction coefficient in RRDE experiment was determine to be 0.37 from the reduction of $Fe(CN)6^{4-/3-}$ redox couple. The ring potential was keep at 1.3 V vs. RHE.

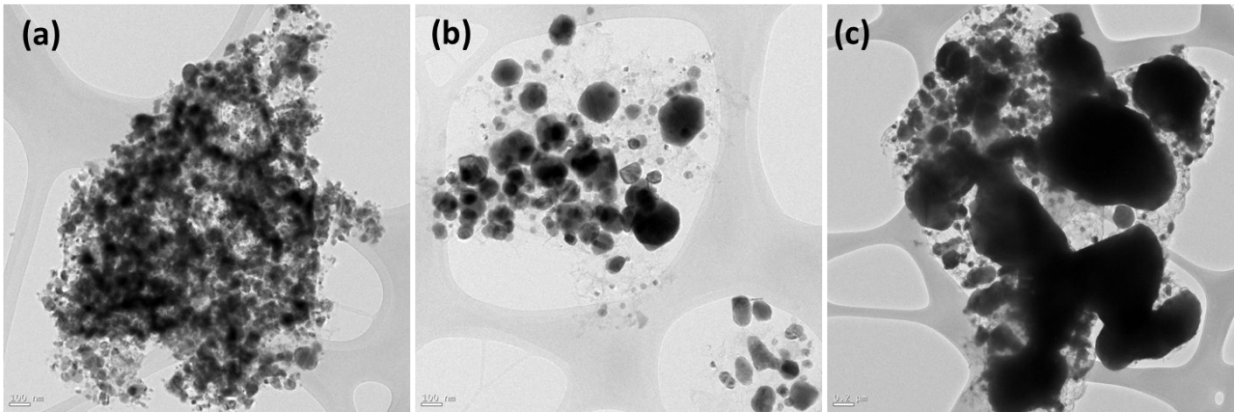

Fig. S1 TEM images of pyrolyzed products obtained at (a) 700˚C, (b) 800˚C and (c) 900˚C.

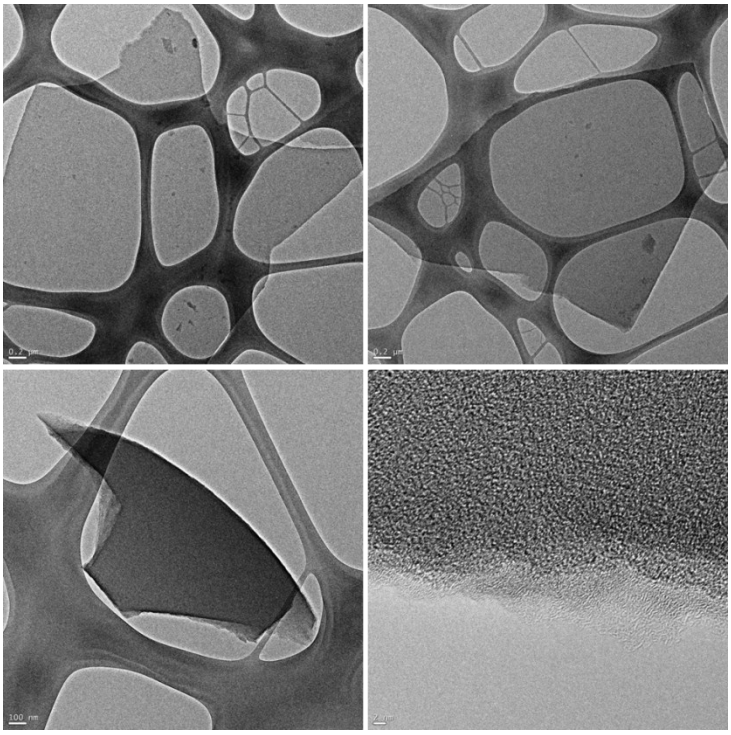

Fig. S2 TEM images of NPC-71 catalyst without using cobalt in the precursor.

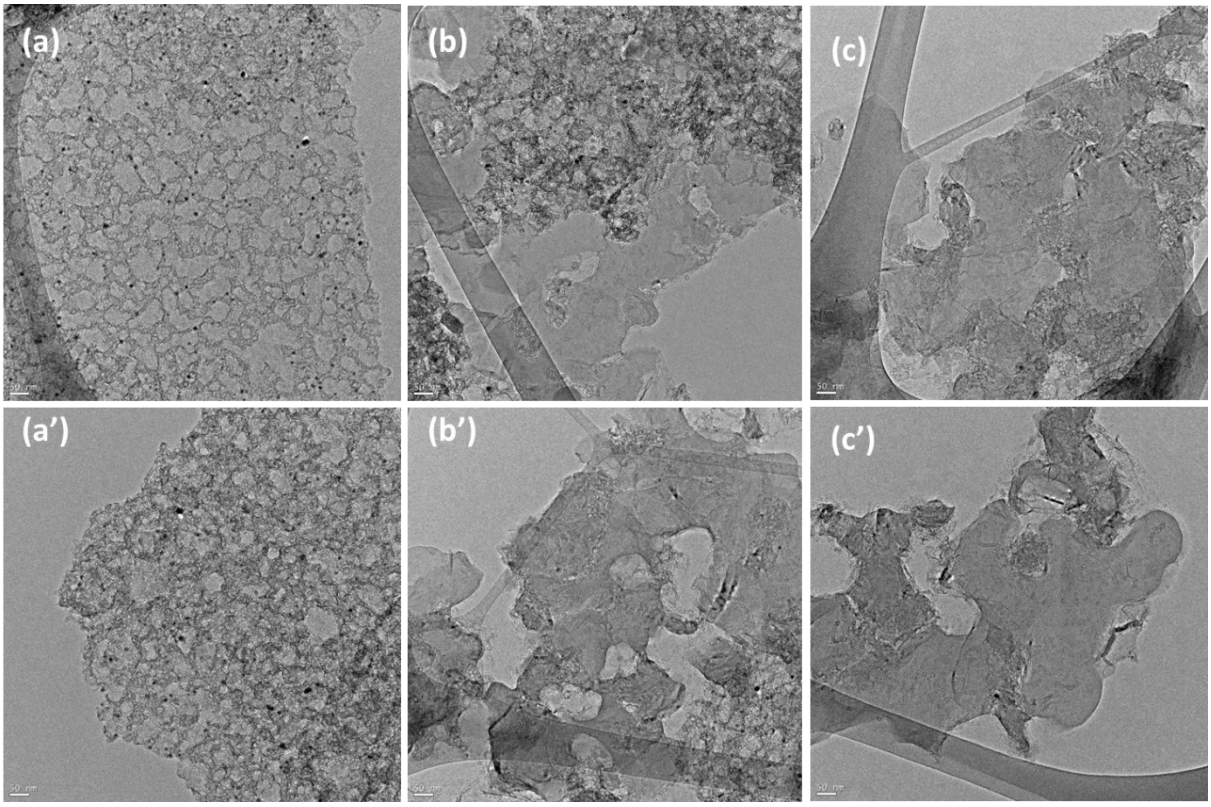

Fig. S3 TEM images of (a, a') CoNPC-71, (b, b') CoNPC-81 and (c, c') CoNPC-91 catalyst.

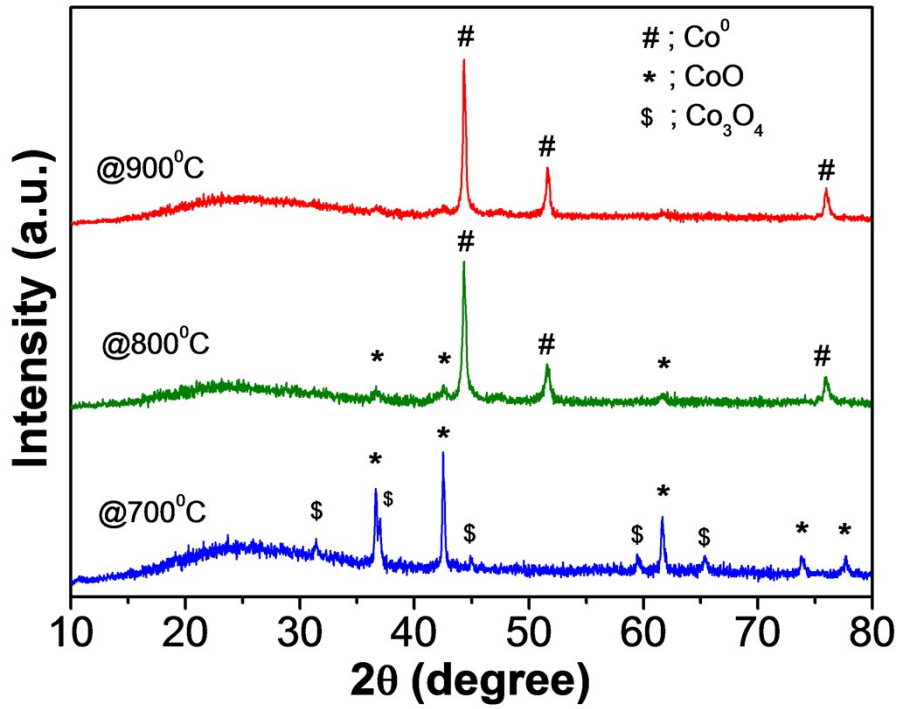

Fig. S4 XRD patterns of as-synthesized products (before acid treatment).

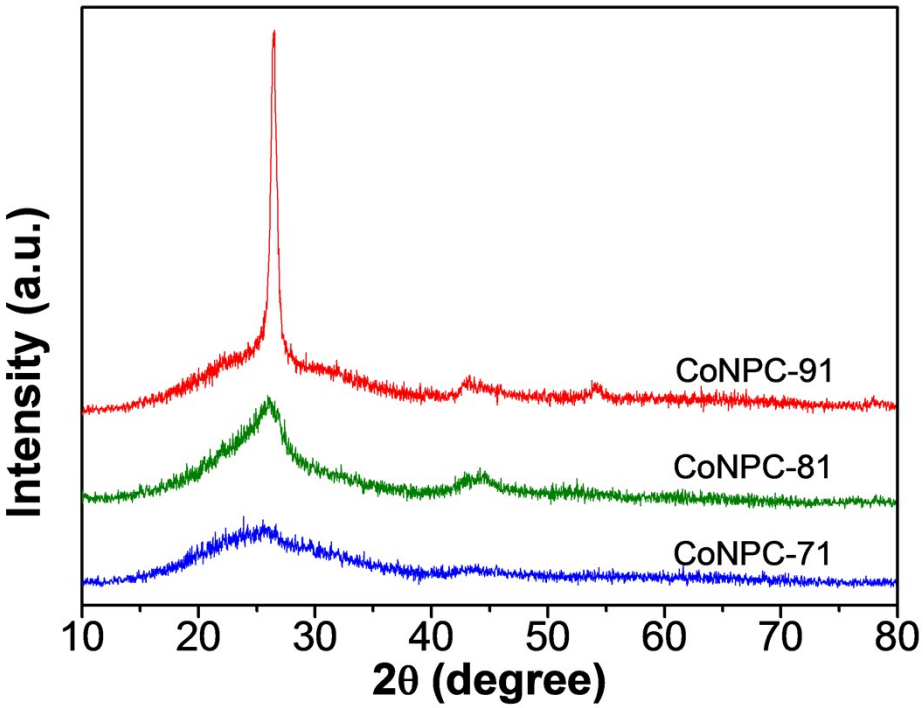

Fig. S5 XRD patterns of CoNPCs catalysts.

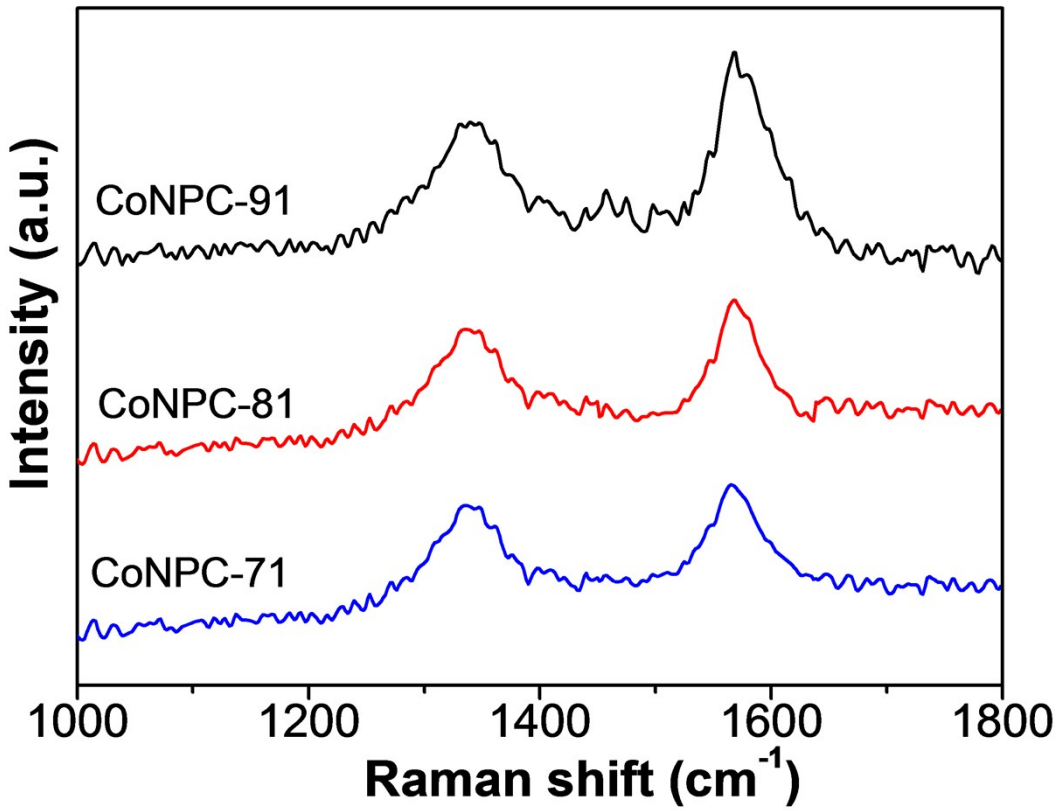

Fig. S6 Raman spectra of CoNPCs catalysts.

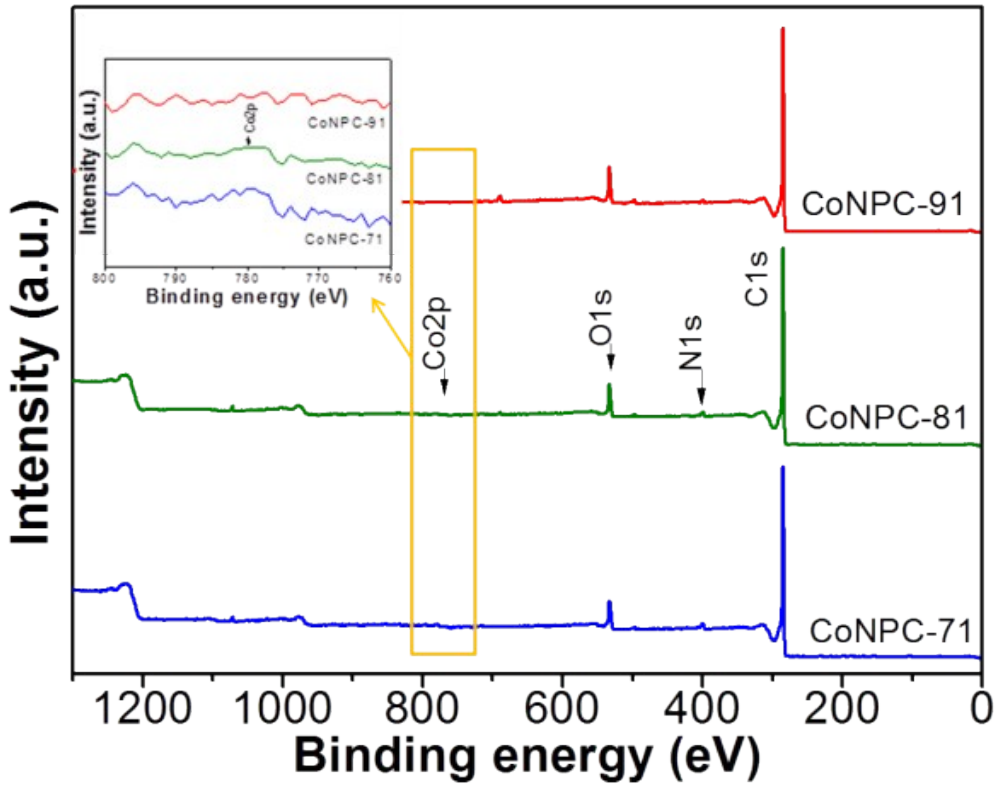

Fig. S7 XPS survey spectra of CoNPCs catalysts. Inset shows a partial high-resolution magnified view of Co2p.

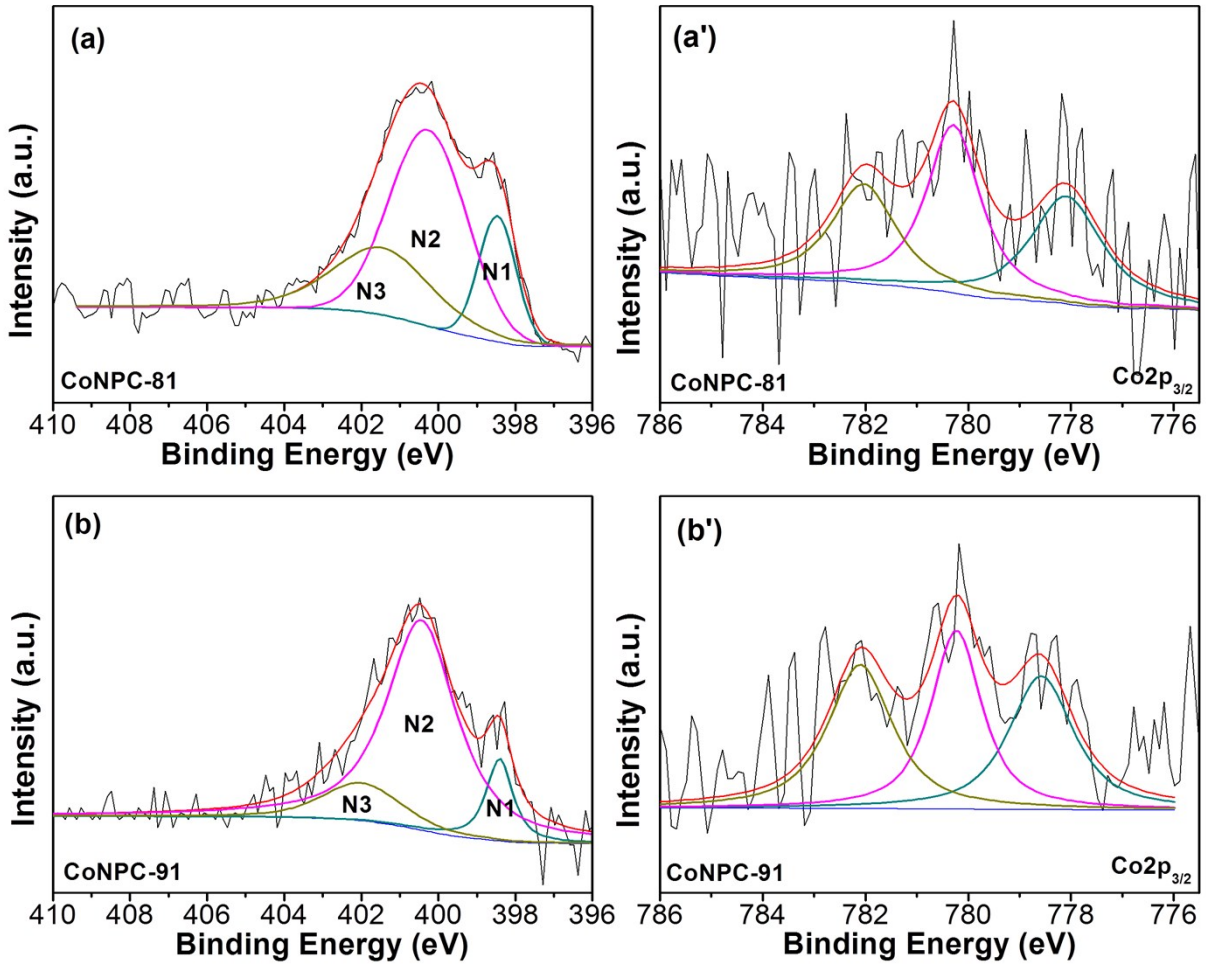

Fig. S8 High resolution XPS of N1s spectra for (a) CoNPC-81 (b) CoNPC-91 and $Co2p_{3/2}$ spectra of (a') CoNPC-81 (b') CoNPC-91 catalyst.

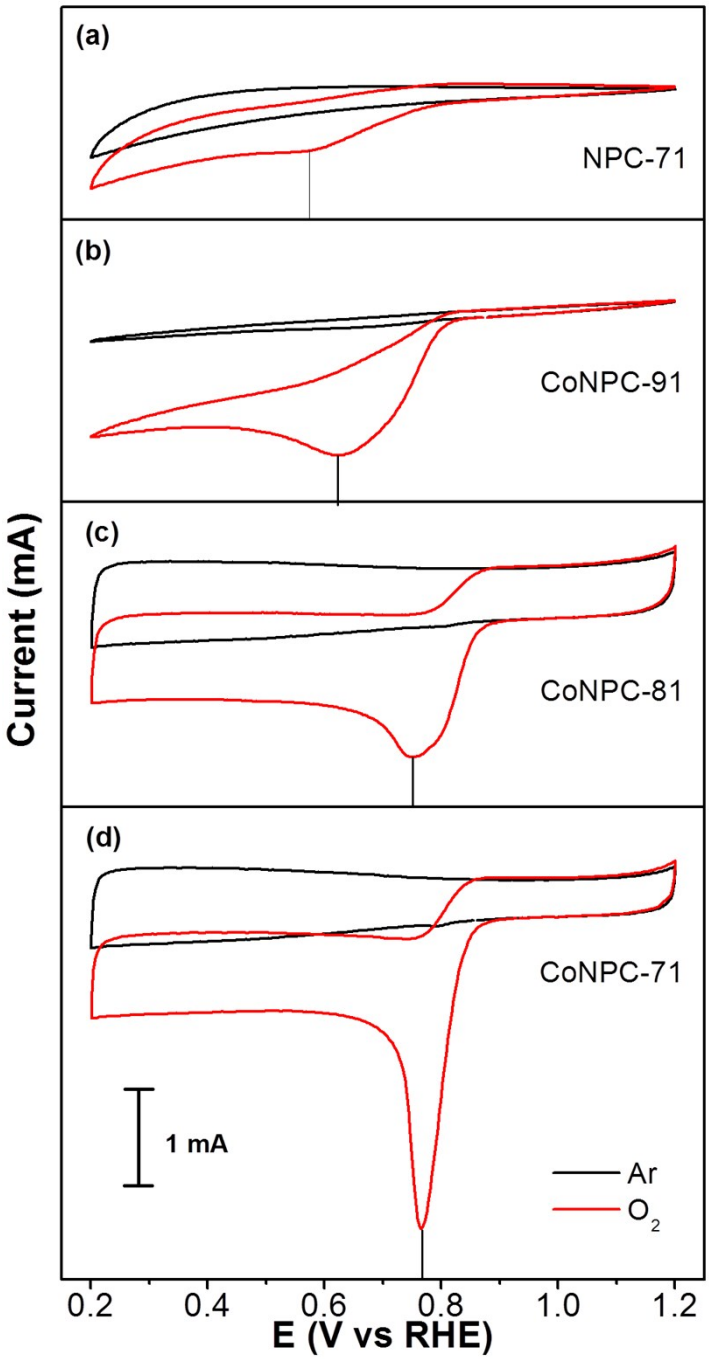

Fig. S9 CVs curves of (a) NPC-71, (b) CoNPC-91, (c) CoNPC-81 and (d) CoNPC-71 on glassy carbon electrode in Ar and O_2-saturated 0.1M KOH; peak position are shown as vertical line (solid black line).

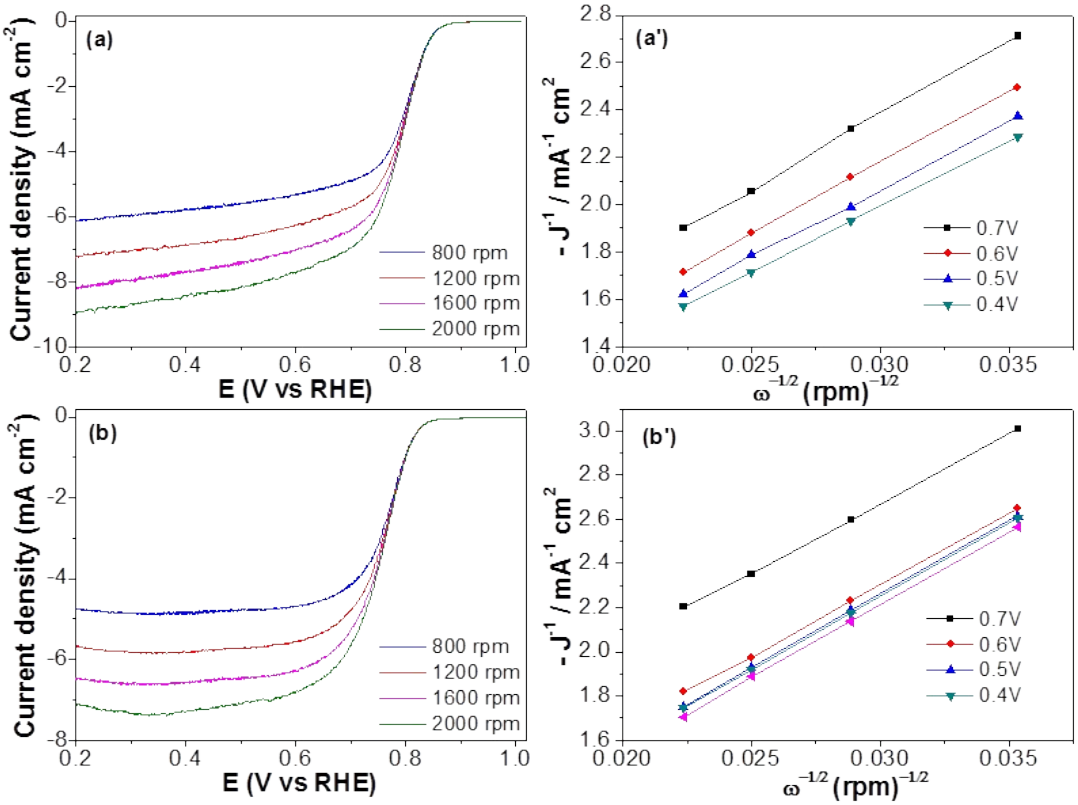

Fig. S10 ORR polarization curve and K-L plot of (a, a') CoNPC-81 and (b, b') CoNPC-91, respectively.

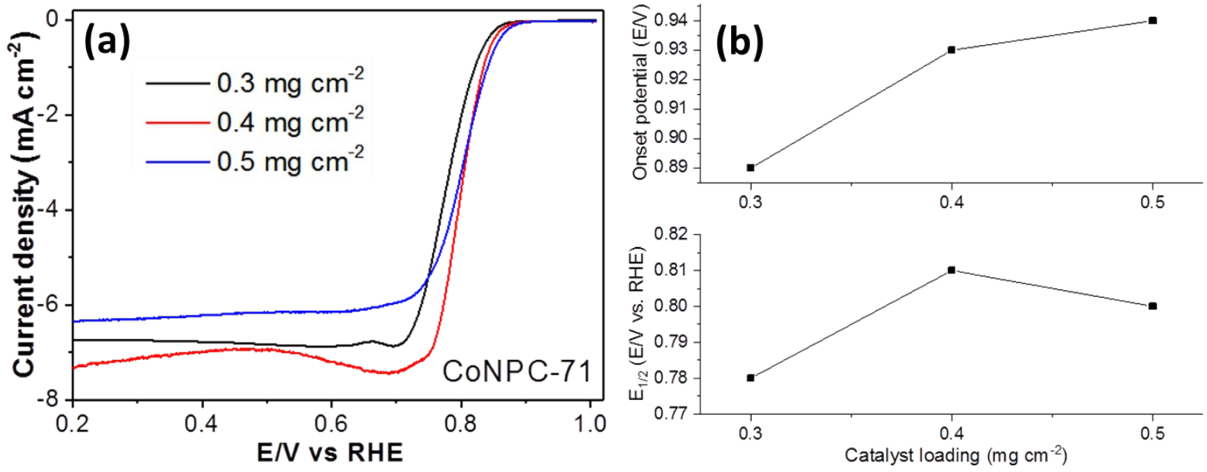

Fig. S11 (a) ORR Polarization curves of CoNPC-71 catalyst with respect to the various catalyst loading from the range of 0.3 to 0.5 mg cm^{-2} obtained from RDE measurement in O_2-saturated 0.1M KOH at a sweep rate 10mVs^{-1}, 1600 rpm, (b) trends in ORR activity, particularly onset potential and half-wave potential ($E_{1/2}$) as a function of mass loading of CoNPC-71 catalyst.

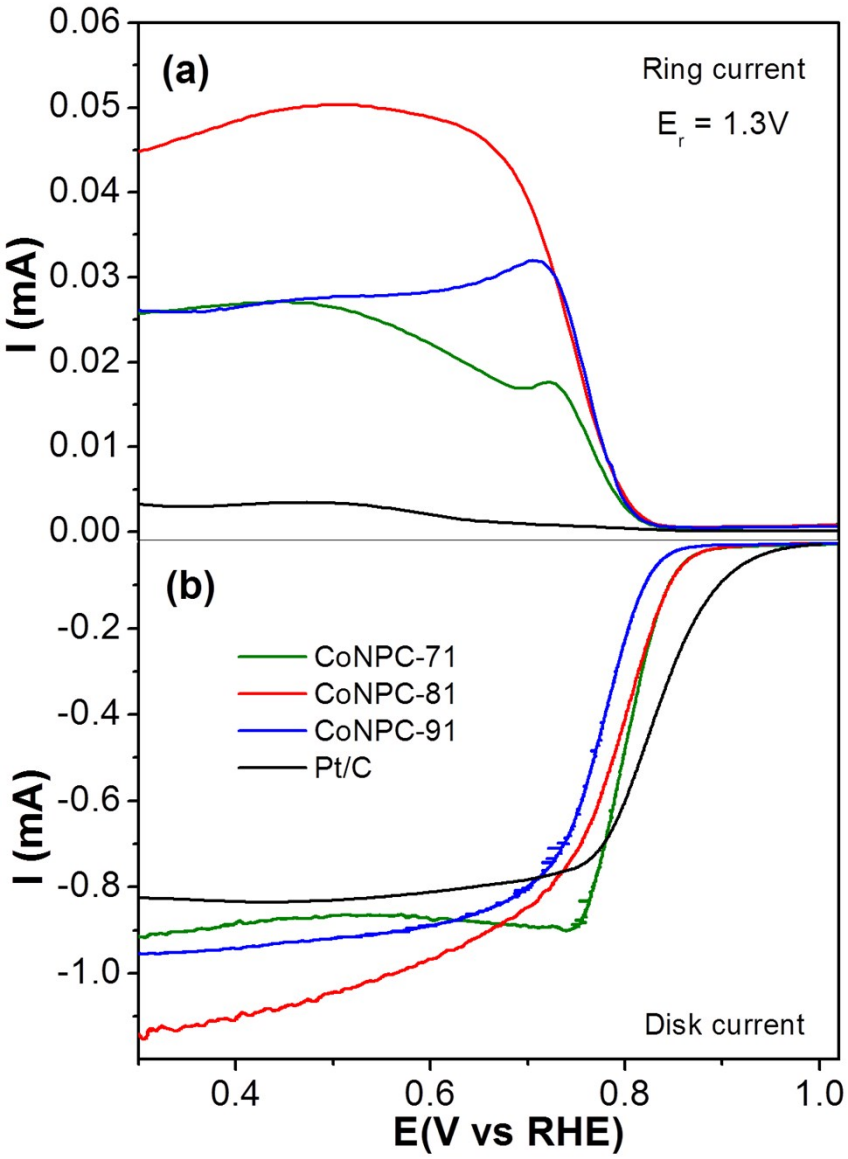

Fig. S12 RRDE response of CoNPC-71, CoNPC-81, CoNPC-91 and Pt/C catalysts obtained at 1600 rpm in O_2-saturated 0.1 M KOH. (Catalyst loading: 0.4 mg cm^{-2} and Pt/C: 30 µg cm^{-2}).

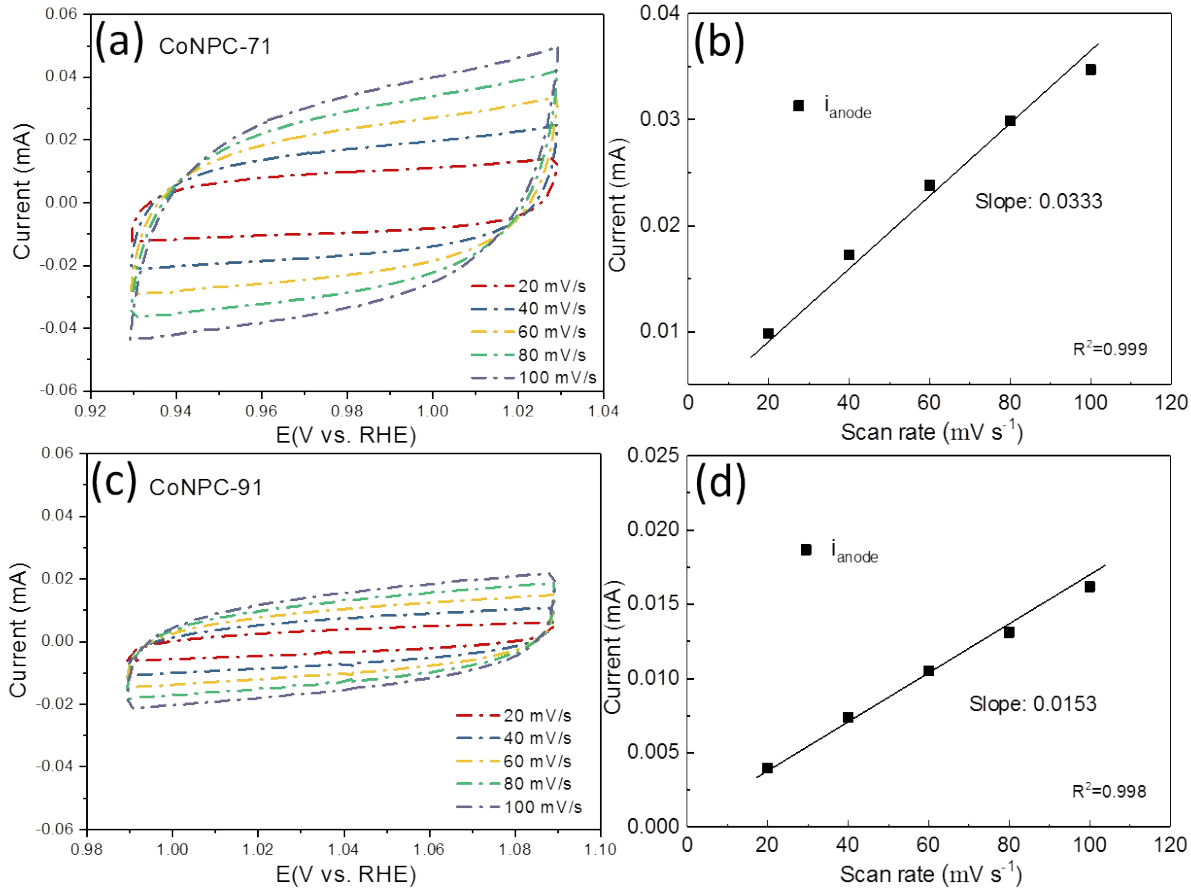

Fig. S13 Electrochemical surface area (ESCA) from the correlation between the current and different scan rates from 20 to 100 mVs^{-1} via CVs: (a,b) CoNPC-71 and (c,d) CoNPC-91 electrocatalysts.

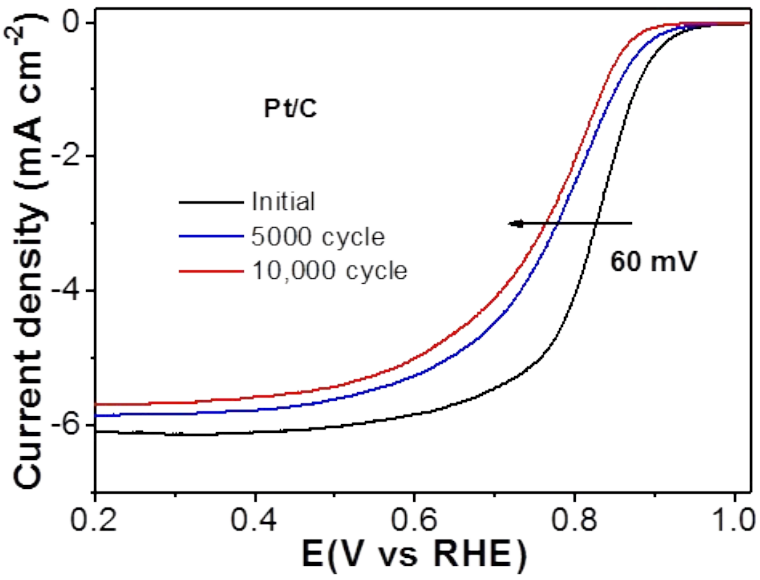

Fig. S14 LSVs of Pt/C during cycling durability test (Cycling test was performed in range of 0.6-1.0 V vs RHE with 50 mVs^{-1}).

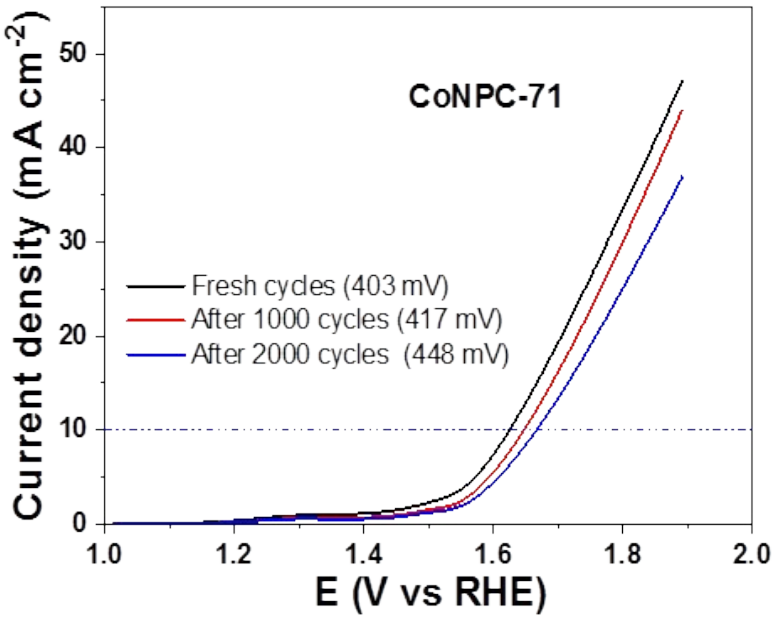

Fig. S15 OER potential cycling tests of CoNPC-71 (Cycling test was performed in a range of 0.8-1.8 V vs RHE with 50mVs^{-1}).

Table. S1 The physical and electrochemical properties of CoNPCs

Catalyst	N1s Distribution (wt%)			Total N content (wt%)	Co2p $_{3/2}$ Distribution (wt%)			Total Co content (wt%)	N/C ratio (wt%)
	N1	N2	N3		Co^0	Co-O	Co-N_x		
CoNPC-71	1.5	3.05	1.1	5.65	0.20	0.45	0.25	0.9	0.019
CoNPC-81	1	2.74	1.1	4.84	0.25	0.27	0.3	0.82	0.017
CoNPC-91	0.3	1.74	0.3	2.34	0.24	0.39	0.22	0.85	0.014

Table. S2 The electrocatalytic activities towards the ORR in 0.1 M KOH electrolyte of CoNPCs catalysts with other reported electrocatalysts.

Electrocatalyst	Onset potential (E/V)	Half-wave potential, $E_{1/2}$ (E/V vs. RHE)	Limiting current density (mA cm^{-2})	Ref.
NPC-71	0.82	0.52	-4.07	This work
CoNPC-71	**0.93**	**0.81**	**-7.48**	**This work**
CoNPC-81	0.93	0.79	-8.30	This work
CoNPC-91	0.87	0.75	-6.75	This work
FeNi-N-CNFs	0.90	0.79	~ -4.0	[S1]
HNCS71 (Fe-N-C)	0.97	0.82	-6.50	[S2]
Co_4N/CNW/CC	~0.90	0.80	-12.35	[S3]
NiCo@GC-600	0.90	0.81	-4.75	[S4]
Fe-N/C-800	0.923	0.809	-6.0	[S5]
Co@Co3O4@C-CM	0.93	0.81	~ -4.6	[S6]
NC/Fe (1.00%)	0.85	~0.75	~-5.25	[S7]

Table. S3 The alkaline membrane fuel cells (AEMFCs) performance data electrocatalyst with commercial membrane in H_2-O_2 system, no added back pressurization, with other noble-metal free electrocatalysts.

Cathode material	Operating Temperature (˚C)	Maximum power density (mW cm^{-2})	Refer.
CoNPC-71	**60**	**68**	**This work**
MnO_x-GC	70	98	[S8]
FePc/MWCNT	50	60	[S9]
NpGr-72	50	27	[S10]
N-CNT	50	37.3	[S11]
Au/C	50	36	[S12]
Ag/C	50	48	[S13]

Table. S4 A comparison of rechargeable Zn-air battery (ZAB) performance with other noble-metal free electrocatalysts.

Catalyst	Current rate (mAcm^{-2})	Charge overpotential (V)	Discharge overpotential (V)	Voltage polarization (V)	Lifetime (number of cycles)	Ref.
CoNPC-91	**10**	**1.96**	**1.15**	**0.81**	**120**	**This work**
40% Pt-Ru	10	2.20	0.91	1.29	60	This work
C-Fe-UFR	10	~2.15	~1.23	~0.92	100	[S14]
Co_4N/CNW/CC	10	2.00	1.16	0.84	405	[S3]
FeNi/NPC	25	1.94	1.15	0.79	150	[S15]
Fe/N/C@BMZIF	10	1.95	1.13	0.82	100	[S16]

References

[S1] Z. Wang, M. Li, L. Fan, J. Han, Y. Xiong, *Appl. Surface Sci.,* 2017, 401, 89-99.

[S2] J. Sanetuntikul, C. Chuaicham, Y.-W. Choi, S. Shanmugam, *J. Mater. Chem. A,* 2015, 3, 15473-15481.

[S3] F. Meng, H. Zhong, D. Bao, J. Yan, X. Zhang, *J. Am. Chem. Soc.,* 2016, 138, 10226-10231.

[S4] A. Sivanantham, S. Shanmugam, *ChemElectroChem,* 2018, 5, 1937-1943.

[S5] L. Lin, Q. Zhu, A. Xu, *J. Am. Chem. Soc.,* 2014, 136, 11027-11033.

[S6] W.Xia, R. Zou, L. An, D. Xia, S. Guo, *Energy Environ. Sci.,* 2015, 8, 568.

[S7] J. Masa, A. Zhao, W. Xia, M. Muhler, W. Schuhmann, *Electrochimica Acta*, 2014, 128, 271-278.

[S8] J.W. Ng, Y. Gorlin, D. Nordlund, T.F. Jaramillo, *J. Electrochem. Soc.,* 2014, 161, D3105-D3112.

[S9] I. Kruusenberg, L. Matisen, Q. Shah, A.M. Kannan, K. Tammeveski, *Int. J. Hydrogen Energy,* 2012, 37, 4406-4412.

[S10] T. Palaniselvam , M. O. Valappil , R. Illathvalappil, S. Kurungot *Energy Environ. Sci.,* 2014, 7, 1059-1067.

[S11] C. V. Rao, Y. Ishikawa, *J. Phys. Chem. C,* 2012, 116, 4340-4346.

[S12] S. D. Poynton, J. P. Kizewski, R.C.T. Slade, J.R. Varcoe, *Solid State Ionics,* 2010, 181, 219-222.

[S13] J.R. Varcoe, R.C.T. Slade, G.L. Wright, Y. Chen, *J. Phys. Chem. B,* 2006, 110, 21041-21049.

[S14] F. Meng, H. Zhong, J. Yan, X. Zhang, *Nano Research*, 2017, 10, 4436-4447.

[S15] H. Zhong, J. Wang, Q. Zhang, F. Meng, D. Bao, T. Liu, X. Yang, Z. Chang, J. Yan, X. Zhang, *Adv. Sustainable Syst.,* 2017, 1, 1700020.

[S16] M. Wang, T. Qian, J. Zhou, C. Yan, *ACS Appl. Mater. Interfaces*, 2017, 9, 5213-5221.